



UNIVERSITY OF LEEDS

This is a repository copy of *Small molecule inhibition of PD-1 transcription is an effective alternative to antibody blockade in cancer therapy*.

White Rose Research Online URL for this paper:  
<http://eprints.whiterose.ac.uk/124056/>

Version: Accepted Version

---

**Article:**

Taylor, A [orcid.org/0000-0003-2295-2611](https://orcid.org/0000-0003-2295-2611), Rothstein, D and Rudd, CE (2018) Small molecule inhibition of PD-1 transcription is an effective alternative to antibody blockade in cancer therapy. *Cancer Research*, 78 (3). pp. 706-717. ISSN 0008-5472

<https://doi.org/10.1158/0008-5472.CAN-17-0491>

---

©2017 American Association for Cancer Research. This is an author produced version of a paper published in *Cancer Research*. Uploaded in accordance with the publisher's self-archiving policy.

**Reuse**

Items deposited in White Rose Research Online are protected by copyright, with all rights reserved unless indicated otherwise. They may be downloaded and/or printed for private study, or other acts as permitted by national copyright laws. The publisher or other rights holders may allow further reproduction and re-use of the full text version. This is indicated by the licence information on the White Rose Research Online record for the item.

**Takedown**

If you consider content in White Rose Research Online to be in breach of UK law, please notify us by emailing [eprints@whiterose.ac.uk](mailto:eprints@whiterose.ac.uk) including the URL of the record and the reason for the withdrawal request.



[eprints@whiterose.ac.uk](mailto:eprints@whiterose.ac.uk)  
<https://eprints.whiterose.ac.uk/>

## **Small molecule inhibition of PD-1 transcription is an effective alternative to antibody blockade in cancer therapy**

Alison Taylor<sup>1,2</sup>, David Rothstein<sup>3</sup> and Christopher E. Rudd<sup>2,4,5</sup>

<sup>1</sup>Leeds Institute of Cancer & Pathology Wellcome Trust Brenner Building, St James's University Hospital, Beckett Street LEEDS LS9 7TF; <sup>2</sup>Cell Signaling Section, Department of Pathology, Tennis Court Road, University of Cambridge, Cambridge UK CB2 1Q; <sup>3</sup>Thomas E. Starzl Transplantation Institute, University of Pittsburgh School of Medicine, Pittsburgh, PA 15261; <sup>4</sup>Division of Immunology-Oncology Research Center, Maisonneuve-Rosemont Hospital, Montreal, Quebec H1T 2M4, Canada; <sup>5</sup>Département de Médecine, Université de Montréal, Montreal, Quebec H3C 3J7, Canada.

Short title: GSK-3 down-regulation of PD-1 in cancer therapy

Key words: T-cells, glycogen synthase kinase-3, PD-1, Tbet, cancer

Correspondence: Christopher Rudd, Centre de Recherche Hôpital Maisonneuve-Rosemont, Laboratoires Antoine Turmel, Room 305, Polyclinique de l'Hôpital Maisonneuve-Rosemont, 5345, Boulevard de l'Assomption, Montreal, QC, Canada H1T 4B3. Phone: 514-252 3400; E-mail: christopher.e.rudd@umontreal.ca.

### Conflict of Interest

The authors declare no potential conflicts of interest.

### Financial Support

C.E. Rudd was supported by Wellcome Trust 092627/Z/10/Z and a Foundation Award from the Centre de Recherche Hôpital Maisonneuve-Rosemont. C.E. Rudd and A. Taylor were also supported by CRUK grant A20105.

## Abstract

The impact of PD-1 immune checkpoint therapy prompts exploration of other strategies to downregulate PD-1 for cancer therapy. We previously showed that the serine/threonine kinase, glycogen synthase kinase GSK-3 $\alpha/\beta$ , is a central regulator of PD-1 transcription in CD8+ T cells. Here, we show that the use of small molecule inhibitors of GSK-3 $\alpha/\beta$  (GSK-3i) to reduce *pdc1* (PD-1) transcription and expression was as effective as anti-PD-1 and PDL-1 blocking antibodies in the control of B16 melanoma, or EL4 lymphoma, in primary tumor and metastatic settings. Further, the conditional genetic deletion of GSK-3 $\alpha/\beta$  reduced PD-1 expression on CD8+ T cells, and limited B16 pulmonary metastasis to the same degree as PD-1 gene deficiency. In each model, GSK-3i inhibited PD-1 expression on tumor infiltrating lymphocytes (TILs), while increasing *Tbx21* (T-bet) transcription, and the expression of CD107a<sup>+</sup> (LAMP1) and granzyme B (GZMB) on CD8+ T-cells. Lastly, the adoptive transfer of T-cells treated *ex vivo* with a GSK-3 inhibitor delayed the onset of EL4 lymphoma growth to a similar extent as anti-PD-1 pre-treatment. Overall, our findings show how GSK-3 inhibitors that downregulate PD-1 expression can enhance CD8+ T-cell function in cancer therapy to a similar degree as PD-1 blocking antibodies.

## Introduction

The co-receptor programmed cell death 1 (PD-1; PDCD1) is a member of the B7 gene family that negatively regulates T-cell function (1-3). PD-1 is expressed in response to T-cell activation and contributes to the exhaustion of CD8<sup>+</sup> T-cells during chronic infections (4,5). The co-receptor binds to ligands, programmed cell death ligand 1 and 2 (PD-L1/L2), on lymphoid and non-lymphoid cells (6-8). Immune checkpoint blockade with anti-PD-1 or anti-PD-L1 has proven successful in the treatment of human cancers, either alone or in combination with anti-CTLA-4 (9,10). PD-1 expression on tumor-infiltrating CD8<sup>+</sup> T-cells correlates with impaired effector cell function (2,11), while PD-L1 expression on tumors can facilitate escape from the host immune system (3), and can serve as a prognostic factor (12). Recent evidence indicates that recovery of responses from anti-PD-1 blockade depends on the related co-receptor (13-15).

The nature of the intracellular signaling pathways that regulate PD-1 expression on T-cells has been the subject of much interest. *Pdcd1* expression can be positively and negatively regulated by different transcription factors such as nuclear factor of activated T-cells (NFAT), Forkhead box protein O1 (FoxO1), Notch, activator protein 1 (AP1), and Blimp1 (B-lymphocyte maturation protein 1) (16-19). Despite this, the identity of the upstream signaling event(s) that control PD-1 expression has been unclear. We and others previously showed that T-cells are activated by protein-tyrosine kinases p56<sup>lck</sup> and ZAP-70 (20,21). p56<sup>lck</sup> binds to co-receptors CD4 and CD8 (22-24) and phosphorylates immune receptor activation motifs (ITAMs) needed for ZAP-70 recruitment to the TcR-CD3 complex (20,23,25). By contrast, glycogen synthase kinase 3 (GSK-3) is a serine/threonine kinase that is active in resting T-cells, and becomes inactivated with T-cell activation (26,27). Differentially regulated isoforms of GSK-3  $\alpha$  and  $\beta$  differ in their N- and C-terminal sequences and can influence pathways initiated by diverse stimuli. The inactivation of GSK-3 can be mediated by several upstream kinases including protein kinase B (PKB/AKT). In CD4<sup>+</sup> T-cells, GSK-3 promotes the exit of NFAT from the nucleus (28,29). TCR and CD28 ligation phosphorylates and inactivates GSK-3 (30-32), while expression of active GSK-3 $\beta$  inhibits the proliferation of T-cells

(30). Engagement of PKB/AKT and GSK-3 in T-cells operates independently of guanine nucleotide exchange factor VAV-1 (31). Clinical trials using GSK-3 inhibitors have been undertaken in the treatment of type II diabetes and various neurological disorders (27,33-35).

Recently, we reported that the inactivation of GSK-3 $\alpha/\beta$  with small interfering RNAs (siRNAs) and small molecule inhibitors (SMIs) specifically down-regulate PD-1 expression for enhanced CD8<sup>+</sup> CTL function and clearance of viral infections (36). The approach has introduced the possibility that small molecule inhibitors of GSK-3 may be effective in the down-regulation of PD-1 in the treatment of cancer. Here, we show that small molecule inhibitors of GSK-3 are as effective as anti-PD-1 in the control of B16 melanoma and EL4 lymphoma growth in mice. Our findings demonstrate, for the first time, the successful application of a GSK-3 inhibitor for the down-regulation of PD-1 on T-cells in cancer immunotherapy.

## Materials and Methods

### Mice and cells.

C57/Bl6 mice were used alongside OT-1 Tg and Rag2 knockout mice. Spleen cells were treated with a hypotonic buffer with 0.15M NH<sub>4</sub>CL, 10mM KHCO<sub>3</sub> and 0.1mM EDTA, pH 7.2 to eliminate red blood cells before suspension in RPMI 1640 medium supplemented with 10% FCS, 50uM beta-mercaptoethanol, sodium pyruvate, 2 mM L-glutamine, 100 U/ml penicillin and streptomycin (GIBCO). T cells were isolated from tumor infiltrating cells, spleen and lymph node samples by use of T cell purification columns (R&D Systems). In some cases, whole lymphocyte samples were used for flow cytometry to determine PD-1 expression in other cell types. Cells included B16 F10 melanoma and EL4 lymphoma cells (obtained from the ATCC). Each cell line was grown to achieve adequate numbers for freezing, followed by repeated thawing for use in the described experiments. The length and time between thawing and use in experiments was on average 3-4 weeks. The cell lines were authenticated by means cell surface staining and flow cytometry for characteristic markers and by their growth properties as described in the literature. Cell cultures were occasionally tested for mycoplasma (last tested in 2011). The research was regulated under the Animals (Scientific Procedures) Act 1986 Amendment Regulations 2012 following ethical review by the University of Cambridge Animal Welfare and Ethical Review Body (AWERB) Home Office UK PPL No. 70/7544.

### Antibodies and reagents.

The following antibodies were used in experiments; Anti-CD3 (2C11), anti-PD-1 (CD279, J43) and anti-CTLA-4 (9H10) (BioXCell); PD-L1 (E1L3N; Cell Signaling Technology), anti-Granzyme B and anti-T-bet (Abcam plc); anti-GSK-3 $\alpha/\beta$ , CD279 (clone EH12.2H7) coupled FITC and mouse IgG1 FITC control (Biolegend); conjugated antibodies anti-CD8 $\alpha$  (clone, 53-6.7), anti-CD4 (clone, RM4-5), CD44, CD62L, CD25, CD69 (ebioscience). Carboxyfluorescein succinimidyl ester (CFSE)

antibodies alongside PE Annexin V Apoptosis Detection Kit with 7-AAD (BioLegend) was used for viability and proliferation assays. GSK3 inhibitors SB415286 3-(3-chloro-4-hydroxyphenylamino)-4-(2-nitrophenyl)-1H-pyrrole-2,5-dione and AZ1080 (Abcam plc). OVA<sub>257-264</sub> peptide (Bachem Ag).

### **Flow cytometry.**

Flow cytometry of antibody staining of surface receptors was conducted by suspending  $10^6$  cells in 100 $\mu$ l PBS and adding antibody (1:100) for 2hr at 4°C. Cells were then washed twice in PBS and in some cases suspended in 100 $\mu$ l PBS with secondary antibody for a further 1h at 4°C. Cell staining was analyzed on a BD FACS Calibur flow cytometer and by FlowJo software. For intracellular staining, cells were fixed in 4% paraformaldehyde (PFA), permeabilized with 0.3% saponin (Sigma–Aldrich) and stained with the desired antibody in saponin containing PBS for 2hr at 4°C, followed by a secondary Ab incubation where primary antibodies were not conjugated.

### **Quantitative real-time polymerase chain reaction (PCR).**

Single-strand cDNA was synthesized with an RT-PCR kit (Qiagen) according to the manufacturer's instructions. Reverse transcription was performed using the RNA polymerase chain reaction (PCR) core kit (Applied Biosystems). Quantitative real-time PCR used SYBR green technology (Roche) on cDNA generated from the reverse transcription of purified RNA. After preamplification (95°C for 2 min), the PCRs were amplified for 40 cycles (95°C for 15s and 60°C for 60s) in a sequence detection system (PE Prism 7000; Perkin-Elmer Applied Biosystems). The exponential phase, linear phase and plateau phase of PCR amplification were carefully monitored to ensure a measurement of real time transcription (33). mRNA expression was normalized against GAPDH expression using the standard curve method. PD-1-FW, 5-CCGCCTTCTGTAATGGTTTGA-3; PD-1-RV, 5-GGGCAGCTGTATGATCTGGAA-3; Tbet-FW, 5-GATCGTCCTGCAGTCTCTCC-3; Tbet-RW, 5-AACTGTGTTCCCGAGGT GTC-3; GAPDH-FW, 5-CAACAGCAACTCCCACTCTTC-3; GAPDH-RW, 5- GGTCCAGGGTT TCTTACTCCTT-3

### **Melanoma lung tumor establishment in wild type mice.**

B16 melanoma cells ( $2 \times 10^5$  taken from the log phase of *in vitro* growth) OVA-peptide pulsed or non-pulsed) were transferred intravenously into syngeneic C57BL/6J mice 10–12-weeks old. The lungs were removed 14 days after the transfer, and visible metastatic colonies on the lungs were counted. In some cases, live imaging used B16 cells tagged with luciferase. Mice were injected intraperitoneally with luciferin (2 ug per mouse), anaesthetized with isoflurane and scanned with an IVIS Lumina (Caliper Life Sciences).

### **Microarray data**

There is no microarray data in the paper.

### **Adoptive transfer of *in vitro* generated cytolytic T-cells (CTLs).**

*In vitro* generated T-cells were injected into mice with 7 day established EL4 tumors. For this, OT-1 CTLs were generated *in vitro* as previously described (36). Primary mouse T cells were isolated using T-cell purification columns (R&D Systems). OVA-specific CD8<sup>+</sup> cytolytic T-cells were generated by incubating OT-I splenocytes with SIINFEKL peptide of OVA (OVA<sub>257-264</sub>) at 10 ng/mL for 5–7 days. Isolated T-cells ( $10^5$  cells) were injected i.v. into mice with established EL4 tumors that had been intra-dermally injected into mice 7 days before cell transfer.

### **Intradermal tumor establishment.**

EL4 or B16 tumor cells were taken from the log phase of *in vitro* growth (approx.. 70% confluency). In some cases where stated, cells were pulsed with OVA peptide for 1hr at 37°C). They were then washed and injected into mice (typically  $3 \times 10^6$  cells for EL4 and  $2 \times 10^5$  for B16 cells). Tumors were clearly visible after 1 week and grew progressively in an encapsulated fashion. Induced tumors were measured on a daily basis using a vernier caliper. Tumors, spleens and lymph nodes

were harvested as indicated, either on day 10 or when the tumor reached a maximum diameter of 12mm. PCR and flow cytometry were performed.

### **Isolation of tumor infiltrating lymphocytes (TILs).**

Solid tumors or nodules from lungs were harvested from mice at the time indicated. Tissue was disrupted using a blade and then incubated in HBSS solution containing 200units/ml of collagenase at 37°C for 2 hrs. Tissue was then passed through a strainer and cells collected and layered onto ficoll before centrifugation. Tumor infiltrating cells were then collected from the lymphocyte layer.

### **Statistical analysis.**

The mean and SE of each treatment group were calculated for all experiments. The number of samples is indicated in the figure legends. Unpaired Student's t tests or ANOVA tests were performed using the InStat 3.0 software (GraphPad). In certain instances, statistics were done using 2-way ANOVA, or by non-parametric Mann Whitney at each time point. \*  $P < 0.05$ , \*\*  $P < 0.01$ , \*\*\*  $P < 0.001$ .

## Results

### GSK-3 inhibits the growth of intravenous and intradermal injected tumors.

To assess whether the down-regulation of PD-1 by GSK-3 inhibition (GSK-3i) was effective in limiting tumor growth, B16 tumor cells were injected intravenously into C57/b6 mice with the GSK-3 inhibitor SB415286 and/or anti-PD-1 (**Fig. 1A**). The optimal dose of SB415286 and anti-PD-1 established in this model was 200ug and 100ug/injection/mouse, respectively. The SMI or antibody was administered every two days following the injection of tumor, followed by a harvest of lungs on day 14 and an assessment of numbers of B16 nodules. GSK-3 inhibitor SB415286 reduced the number of B16 spots from a mean of 145 to 60 (i.e. >55% inhibition). This effect was comparable to anti-PD1 which showed a mean of 70 spots (i.e. >50% inhibition). Further, the combination of SB415286 and anti-PD-1 had the same effect as SB415286 and anti-PD-1 individually (n=6). Flow cytometry confirmed that GSK-3i reduced PD-1 expression on T-cells from the tumor (i.e. tumor infiltrating (TILs), spleen and draining lymph nodes (**Fig. 1B**). By contrast, no effect on the expression of other receptors such as CD3, CD8, CD44, CD62L, CD25 and CD69 was observed (**Supplementary Fig. S1A**), similar to previous results involving GSK3i in viral infection (**36**). GSK-3i reduced *pcdc1* (PD-1) transcription in T-cells from isolated spleen of tumor bearing mice (i.e. 3.7 to 0.8), concurrent with an increase in *Tbx21* (Tbet) transcription (i.e. 1.6 to 4.2) (**Fig. 1C**). Concurrent with reduced tumor growth, SB415286 treatment increased the % of CD8<sup>+</sup> TILs expressing CD107a<sup>+</sup> (Lamp1) and granzyme B (GZMB) (i.e. mean % of 14 to 23), indicative of an increased presence of CD8<sup>+</sup> killer T-cells in the tumor mass (**Fig. 1D**). These data showed that the down-regulation of PD-1 with a small molecule inhibitor of GSK-3 can be as effective as anti-PD-1 in the control of B16 pulmonary metastasis in mice.

We also examined the effect of SB415286 doses on the growth of B16 cells tagged with luciferase (**Fig. 1E**). At day 14, mice were injected intraperitoneally with luciferin and scanned by IVIS Lumina imaging. SB416286 reduced the luciferase signal at 100 and 200ug/mouse, the dose of 200ug being more effective (left panels). In terms of T-cell subsets, both doses reduced PD-1

expression on the surface of CD8<sup>+</sup> cells (right panels). By contrast, PD-1 expression was reduced to a lesser extent on CD3 negative NKp46<sup>+</sup> NK cells. No reduction on NK cells was observed at 100ug, despite the ability of this dose of drug to reduce tumor burden. Further, we found that PD-1 expression on CD4<sup>+</sup> T-cells, and CD4<sup>+</sup> CD25<sup>+</sup> FoxP3<sup>+</sup> PD-1<sup>+</sup> regulatory T-cells (TRegs) taken from tumors was unaffected. These data showed that GSK-3i preferentially down-regulated PD-1 on CD8<sup>+</sup> T-cells, while having a lesser effect on NK cells and no obvious effect on CD4<sup>+</sup> T-cells in the B16 tumor model. In a comparison of injection frequency, more frequent injections of 200 or 400ug was optimal (**Supplementary Figure S1B**). 4 to 6 injections of each dose seemed optimal for tumor rejection and PD-1 down-regulation *in vivo*. 200ug was as effective as 400ug in these setting.

To assess the role of GSK-3 genetically, we next compared B16 tumor growth in *GSK-3 $\alpha/\beta$*  conditional knock out mice relative to wild-type and PD-1 deficient mice (*Pdcd1*<sup>-/-</sup>). *GSK-3 $\alpha/\beta$*  conditional knockout (*GSK-3 $\alpha/\beta$* <sup>-/-</sup>) mice were generated from a GSK-3 alpha flox/flox/beta flox/flox Lck Cre<sup>+</sup> parental mice (parental line kindly provided by Dr. Jim Woodgett, U of Toronto). T-cells from conditional knockout *GSK-3 $\alpha/\beta$* <sup>-/-</sup> mice showed the expected reduction in PD-1 expression on CD8<sup>+</sup> T-cells when assessed from mice injected with B16 cells and assayed on day 10 (**Fig. 2A**, left panel). By contrast, no effect on PD-1 expression on CD4<sup>+</sup> T-cells was noted, either in terms of cell number, or mean fluorescent intensity (MFI) (right panel). Secondly, B16 pulmonary metastasis was markedly reduced in *GSK-3 $\alpha/\beta$* <sup>-/-</sup> mice (**Fig. 2B**). Intriguingly, the tumor growth in *GSK-3 $\alpha/\beta$* <sup>-/-</sup> mice was reduced to a similar extent as seen in *Pdcd1*<sup>-/-</sup> mice (i.e. from 110 spots to <10 in both sets of mice) (**Fig. 2C**). Further, the injection of anti-PD-1 in *GSK-3 $\alpha/\beta$* <sup>-/-</sup> mice had no further effect on the number of nodules in lungs (**Fig. 2B**, upper inset). Conversely, the injection of SB415286, or another GSK-3 inhibitor, AZ1080 in *Pdcd1*<sup>-/-</sup> mice had no additional effect in reducing the number of nodules (**Fig. 2C**, upper inset). Overall, the data showed that GSK-3 inhibitor preferentially down-regulated PD-1 expression on CD8<sup>+</sup> T-cells and that the loss or inhibition of SB415286 and PD-1 in mice had the same effect in limiting B16 pulmonary metastasis. This observation, combined with the finding that GSK-3 inhibitors had no further inhibition of tumor growth in *Pdcd1*<sup>-/-</sup> mice, and that

anti-PD-1 had no further effect on tumor growth in *GSK-3 $\alpha/\beta$* <sup>-/-</sup> mice supported the notion that GSK-3 inhibition operated to limit tumor growth primarily via the down-regulation of anti-PD-1.

To further exclude that SB415286 had a direct effect on tumor cells, the SMI was injected into *Rag2*<sup>-/-</sup> mice (missing B and T-cells) with the B16 tumor (**Fig. 2D**). Under this condition, SB415286 had no effect on limiting tumor growth. In addition, carboxyfluorescein succinimidyl ester (CFSE) labelled B16 cells were co-cultured of SB415286 *in vitro* over 5 days and assessed for differences. SB415286 had no obvious effect on the growth of B16 cells (**Supplementary Fig. S2**). Taken together, these data was most consistent with the interpretation that protective effects of GSK-3i was due primarily to an effect on CD8<sup>+</sup> T-cells.

We next also assessed whether the SMI SB415286 could affect PD-1 expression on human T-cells (**Supplementary Fig. S3**). Human CD4<sup>+</sup> CD8<sup>+</sup> T cells isolated from human peripheral blood were stimulated with anti-CD3/CD28 for 72hs prior to resting overnight and then incubated with SB415286 for various times and stained by flow cytometry for PD-1 expression. The SMI reduced the % of cells expressing PD-1 by >55% and the mean fluorescent intensity (MFI) for expression by >65% for cells when assayed at 48 hours (left upper and lower panels). Lesser inhibition was also apparent at >96 hours. See examples in right panels at 10min, 24 and 48 hours (right panel). As a control, the expression of CD3, CD4 and CD8 was unaffected. These data confirm that GSK-3i can be used to down-regulate PD-1 on CD3<sup>+</sup>CD8<sup>+</sup> human T-cells.

SB415286 and anti-PD-1 had similar effects on the growth of more established B16 pulmonary metastases in mice (**Fig. 3A**). B16 tumor cells were injected intravenously and left for 7 days before beginning treatment. Lungs were harvested on day 19, and assessed for B16 nodules. Due to the extended time, non-treated animals showed larger nodules than seen in the previous experiments. Despite this, injection of mice with either SB415286 and anti-PD-1 greatly reduced the number of nodules from 135 to 5-20. Both reagents also reduced the size of the remaining nodules from a mean of 3 to 0.05mm in diameter. Further, the combined injection of SB415286 and anti-PD-1 reduced the number of spots to the same extent as each individual treatment (i.e. 5-10).

As a control, qPCR measurements confirmed the reduction in *pdcd1* transcription, with a concurrent increase in *Tbx21* transcription in splenic T-cells (**Fig. 3B**). This reduction in PD-1 expression was confirmed by flow cytometry where we observed that SB415286 or combined therapy reduced PD-1 expression in T-cells from spleen and TILs (**Fig. 3C**). Further, this reduction in expression correlated with an increase in Lamp1 and GZMB expressing CD8<sup>+</sup> TILs (**Fig. 3D**).

We next investigated whether GSK-3 inactivation was also as effective as anti-PD-1 checkpoint blockade in the control of the growth of solid B16 tumors. For this, B16 cells were injected intra-dermally, followed by intra-peritoneal injections of either SB415286 or anti-PD-1 (**Fig. 4A**). We found that SB415286, anti-PD-1 and the combination slowed tumor growth such that 10mm sized tumors were not seen until days 19-22, rather than day 14 in untreated mice. Further, SB415286 or anti-PD-1 increased overall survival to the same general extent, as seen in the Kaplan-Meier survival plot with a 40-50% survival at day 30 (**Fig. 4B**). As a control, qPCR of isolated spleen T-cells showed a marked decrease in *pdcd1* transcription, while increasing the transcription of *Tbx21* (**Fig. 4C**). Flow cytometry also showed a decrease in PD-1 expression in T-cells from the spleen and extracted TILs (n=5) (**Fig. 4D**). Reduced *Pdcd1* and increased *Tbx21* transcription was also observed in TILs (**Fig. 4E**). Lastly, both SB415286 and combination therapy increased the numbers of CD107a<sup>+</sup>GZMB<sup>+</sup>CD8<sup>+</sup> cells indicative of the increased presence of more effective killer T-cells (**Fig. 4F**). There was no significant difference between the number of CD107a<sup>+</sup>GZMB<sup>+</sup>CD8<sup>+</sup> cells with SB415286 versus SB415286 and anti-PD-1.

We also assessed the effect of GSK-3 inactivation on immune cell rejection of another tumor model, EL4 lymphoma cells (**Fig. 5**). Priming of OT-1 OVA-specific T cells with SIINFEKL peptide of OVA (OVA<sub>257-264</sub>) produces a specific CTL response against tumor targets (37). EL4 cells were pre-treated with 0, 2, 5 and 10ug of OVA peptide, and washed, prior to injection. EL4 cells not exposed to peptide were injected into the left flank of OT-1 Tg mice, while those exposed to peptide were injected into the right flank. SB415286 was injected intra-peritoneally on day 0, and tumor growth

was then monitored over 10 days before harvesting (**Fig. 5A**, upper panel). Tumor size was reduced especially with 5 and 10ug OVA peptide; however, tumors were still evident at all peptide concentrations (lower panels). By contrast, in 4/7 experiments, SB415286 treatment resulted in a complete loss of tumor mass at all peptide concentrations in > 80% of mice. This remarkable tumor clearance was observed in mice of different ages, 4-6 weeks (**Supplementary Fig. S4A**), 6-10 weeks (**Supplementary Fig. S4B**) and 6 months (**Supplementary Fig. S4C**). As a control, real time PCR of splenic T-cells confirmed SB415286 *in vivo* injection inhibited *pcdc1* transcription, while increasing *Tbx21* transcription (**Fig. 5B**). Flow cytometry staining of cells with anti-PD-1 also confirmed the reduction in co-receptor expression. In experiments where the tumors were not eliminated by SB415286 at all peptide concentrations, the drug and anti-PD-1 had similar effects (**Fig. 5C**). At 5ug/ml OVA, untreated mice carried tumors of 5mm by day 14, while SB415286, anti-PD-1, or the combination, delayed the appearance of this sized tumor until day 20-22. Similarly, in the case of mouse survival, at 2ug/ml OVA peptide, the SMI SB415286, anti-PD-1 and combination therapy increased survival from 17 to 24-26 days as seen by the Kaplan-Meier survival plot (lower panel). At 5ug/ml OVA, SB415286, anti-PD-1 and combination therapy increased survival from 21 to 30-31 days. At 10ug/ml OVA peptide, SB415286 and anti-PD-1 completely protected against death, compared to day 25 for untreated mice. As an additional control, flow cytometric analysis of intracellular/surface stained cells showed that SB415286 treatment did not affect the expression of other markers (i.e. other than PD-1) such as CD44, CD4, FasL, FoxP3, CD152 (CTLA-4) and CD25 (**Supplementary Fig. S5**).

In another approach, we assessed PD-1 blockade using a blocking antibody to the PD-1 ligand (PD-L1) (**Fig. 5D**). SB415286, anti-PDL-1 and anti-PD-1 delayed the onset of EL-4 tumor growth at 5ug OVA peptide from an onset of growth from day 10 to 20-21 (upper left panel). At 10ug OVA, SB415286, anti-PDL-1 and anti-PD-1 completely eradicated the presence of tumors (upper right panel). Again, as a control with 5ug peptide, SB415286 markedly reduced in *pcdc1*

transcription while increasing Tbet expression. These studies showed SB415286, anti-PDL-1 and anti-PD-1 were remarkably similar in delaying the onset of tumor growth.

We then compared the effect of GSK-3 inactivation versus anti-PD-1 on EL4 solid tumors in the absence of OVA peptide (**Fig. 6**). This required co-injections of SB415286 and/or anti-PD-1 as depicted (**Fig. 6A**) and an assessment of tumor growth over a longer period of 40 days. EL4 tumors grew to 10mm by day 5 in untreated mice, which was prolonged to day 12 in SB41528 and anti-PD-1-treated mice (lower panel). The tumor completely regressed in one to three mice by day 18 with anti-PD-1, or the combination of SB41528 and anti-PD-1. The cooperative effect of combination therapy was also reflected in survival (**Fig. 6B**). While untreated mice died by 11 days, 50% of mice on combined therapy remained alive by 40 days as shown in the Kaplan-Meier survival plot. Flow cytometry of T-cells isolated from the spleens, draining lymph nodes and TILs demonstrated lower expression levels of PD-1 (**Fig. 6C**). This was confirmed with PCR demonstrating a reduction in *Pdcd1* and an increase in *Tbx21*(**Fig. 6D**).

To determine the duration of the effect of SB415286, PD-1 expression was monitored in mice co-injected with EL-4 tumors and a single injection of the drug (**Supplementary Fig. S6**). Mice were sacrificed at various times and PD-1 expression on spleen CD3+CD8+ T-cells was assessed by flow cytometry. The effects on PD-1 expression on CD3+CD8+ T-cells was sustained until 7-10 days (i.e. 57% suppression at day 5; 42% at day 7) with expression returning to control levels from day 10-14 (i.e. 22% suppression at day 10 and 7% at day 14). These data indicate that the effects of SB415286 was sustained for over 7-10 days.

Lastly, we tested whether pre-treatment of T-cells *ex vivo* with SB415286 provided protection (**Fig. 7**). EL4 cells were intra-dermally injected into mice for 7 days followed by the transfer of OT-1 CTLs that had been cultured *in vitro* for 7 days in the absence or presence of OVA peptide plus the SMI SB415286 or anti-PD-1. The transfer of cells without any SB415286 or anti-PD-1 pre-treatment delayed the onset of growth at all peptide concentrations (**Fig. 7A**). However, pre-treatment with

SB415286, anti-PD-1 and in combination further slowed tumor growth. At 5ug Ova, each treatment delayed the onset of tumor growth until days 19-21. Further, tumors attained a diameter of 8mm by day 16 and at days 25-27 with SB415286, anti-PD-1 or combined therapy. In this instance, the effect of SB415286 was the same as anti-PD-1. Pre-cultured T-cells (prior to adoptive transfer) showed the expected decrease in *pdc1* transcription while increasing the transcription of *Tbx21* (**Fig. 7B**). Flow cytometry prior to transfer confirmed the reduction in PD-1 expression at different OVA concentrations (**Fig. 7C**). These data showed that the efficacy of GSK-3 inhibition was the result of a direct effect on T-cells, and that the pre-treatment of T-cells *ex vivo* with either anti-PD-1 or SB415286 provided protection against tumor growth.

## Discussion

Immune checkpoint blockade with anti-PD-1 or anti-PD-L1 has proven to be a highly promising treatment of human cancers, either alone or in combination with other reagents such as anti-CTLA-4 (2,9,10). However, only a minority of patients is responsive to this therapy, and there is a need to find alternate ways to complement present approaches. We previously showed that the kinase GSK-3 $\alpha/\beta$  is a central regulator of PD-1 expression and that small molecule inhibitors of GSK-3 (GSK3i) are effective in promoting viral clearance (33). In this paper, we have shown that GSK-3i inhibition of *pdc1* (PD-1) transcription with a small molecule inhibitor (i.e. SB415286) is as effective as anti-PD-1 and PDL-1 blocking antibodies in the control of B16 and EL-4 tumor growth. Our findings identify a potential alternate approach using small molecule inhibition of PD-1 expression in cancer therapy.

Our findings showed that GSK-3 inhibition with SMI treatment operates primarily via a reduction in PD-1 expression on the CD8<sup>+</sup> T-cells. As in the case of drug inhibition of PD-1 transcription, GSK-3 $\alpha/\beta$ <sup>-/-</sup> T-cells showed a reduction in PD-1 expression, while B16 pulmonary metastasis was reduced to a similar extent in *Pdcd*<sup>-/-</sup> and GSK-3 $\alpha/\beta$ <sup>-/-</sup> mice. In each model, GSK-3i inhibited *Pdcd1* transcription and PD-1 expression on tumor infiltrating T-cells (TILs), while increasing *Tbx21* (Tbet) transcription and the presence of CD8<sup>+</sup> TILs expressing CD107a<sup>+</sup> (LAMP1) and granzyme B (GZMB). Despite this, it is also important to note that GSK-3 is likely to affect other aspects of T-cell function in an PD-1 independent fashion. We showed that the enzyme up-regulates T-bet expression (36) which regulates the expression of numerous other genes such as GZMB and IFN $\gamma$ 1 (38). GSK-3i may eventually be found to alter the expression of other receptors and mediators and provide a potential advantage over anti-PD-1 blockade. However, in the context of the models examined to date, the down-regulatory effect on PD1 plays a central role in generating anti-tumor immunity.

The role of the immune system in providing protective immunity via GSK-3 was also seen in conditionally deleted *GSK-3 $\alpha/\beta$* <sup>-/-</sup> mice. Intriguingly, GSK-3 inactivation by gene ablation, or exposure to SMIs, preferentially reduced PD-1 expression on CD8<sup>+</sup> T-cells. Expression on CD4<sup>+</sup> T-cells, and CD4<sup>+</sup> CD25<sup>+</sup> FoxP3<sup>+</sup> PD-1<sup>+</sup> regulatory T-cells (Tregs) from tumors was unaffected. Although NK cells play key roles in eliminating B16 tumors (39-42), PD-1 expression was less affected on this subset than on CD8<sup>+</sup> T-cells. Further, at the lower SMI dose of 100 $\mu$ g, reduced PD-1 expression on NKp46<sup>+</sup> NK cells was not observed, despite the protective effect of the reagent on B16 tumor growth. At a higher dose, some reduction in PD-1 expression was observed, but to a lesser extent than seen on CD8<sup>+</sup> T-cells. Further, SB415286 had no effect on B16 pulmonary metastasis in *Rag2*<sup>-/-</sup> mice which express NK cells. Therefore, while we do exclude an effect on NK mediated killing of tumors (42), the anti-tumor effect of GS3i in our model was primarily due to an effect on CD8<sup>+</sup> T-cells. This latter observation also argued against a direct effect of the SMI on tumor growth. This lack of a direct effect of SMIs on tumors was supported by the absence of an effect of SB415286 on the *in vitro* growth of B16 cells.

In addition to effects on B16 cells, GSK-3 inhibition, anti-PD-1 and anti-PDL-1 had similar effects on EL4 lymphoma solid tumor growth. In most mice, SB415286 treatment eradicated tumors, while in other mice, depending on the concentration of OVA peptide, the SMI delayed the onset of growth by 20-22 days. GSK-3 inhibition, anti-PD-1 or anti-PDL-1 delayed tumor growth to the same extent. Further, the combination of SB415286 and anti-PD-1 had the same effect as monotherapy. Occasionally, we observed some cooperation between anti-PD-1 and GSK-3i in the EL4 model, and therefore, we cannot exclude that future work will show cooperativity dependent on the tumor model.

Lastly, we found that the *ex vivo* pre-treatment of CTLs followed by adoptive cell transfer was effective in the control of tumor growth. As in the other models, SB415286 and anti-PD-1 delayed the onset of growth to the same extent. This experiment confirmed that the protective effect of GSK-

3 on tumor growth was due to an effect on the function of T-cells. Combination therapy did not provide an obvious improvement, supporting the notion that SB415286 was acting to inhibit tumor growth primarily by down-regulating the expression of PD-1. GSK-3 SMIs may therefore have application to cell therapy, potentially to improve chimeric antigen receptor (CAR) therapy (43).

Overall, there are potential advantages and disadvantages to the use of the GSK-3 SMI versus anti-PD-1 antibody therapies. Anti-PD-1 therapy is expensive and associated with adverse effects such as fatigue, rash and possible autoimmune complications such as colitis. Although we cannot exclude these inflammatory effects with the use of GSK-3 inhibitors, we have seen no evidence of autoimmunity with SMIs or in the *GSK-3 $\alpha$ / $\beta$ -/-* mice over 2 years. Further, the use of many GSK-3 inhibitors is no longer restricted by patent coverage (27), and SMI inhibition offers the advantage of more accurate dosing, lower cost and the potential of oral administration. Importantly, PD-1 expression on both murine and human T-cells were down-regulated by GSK-3i.

The potential disadvantage of GSK-3 inactivation is a possible direct effect on the function of other host cells or the tumor itself. However, lithium chloride, an inhibitor of GSK-3, has been used for decades for the treatment of bipolar disease without a reported increase in tumor frequency. The dose of SB415286 inhibitor (200ug per 20g mouse) in our study was roughly comparable to the dose of another inhibitor Tideglusib used in a phase 2 oral study (800mg in a 80kg patient) to treat progressive supranuclear palsy (35). Further, we showed that the effects of GSK-3 SMIs are durable such that a single dose injection of SB415286 down-regulated PD-1 for 10-14 days. Although, we failed to see any effect of SB415286 on the growth of B16 melanoma cells, GSK-3 inhibition has been reported to directly inhibit the growth of multiple myeloma, neuroblastoma, hepatoma and prostate tumors (44-48). It is therefore possible that, in some instances, GSK-3 inhibitors might directly inhibit the growth of some tumors. Despite these possibilities, the major effect of GSK-3i in our studies was amplify the ability of the immune system to react against tumor growth as shown by the effect of *ex vivo* treated T-cells in adoptive cell therapy as well as by the

elimination of tumors in mice where *GSK-3 $\alpha/\beta$*  conditionally deleted in the T-cells. Certain tumors can also impair proximal TCR signaling events as a form of immune avoidance (49,50). The inhibition of GSK-3 could potentially circumvent this impairment given that GSK-3 operates downstream of proximal signal mediators such as p56<sup>lck</sup>. Further work is needed to uncover the full range of downstream effects that may be regulated by GSK-3 regulation in anti-tumor immunity.

## **Acknowledgements**

We thank Dr. Jim Woodgett, Lunenfeld-Tanenbaum Research Institute, Mount Sinai Hospital, Toronto for the heterozygotes of the GSK-3 $\alpha/\beta$  conditional knock-out mice. PD-1 deficient mice (*Pdcd1*<sup>-/-</sup>) were a kind gift of Prof. T. Honjo, Kyoto University Faculty of Medicine, Japan.

## References

1. Schildberg, F. A., Klein, S. R., Freeman, G. J., and Sharpe, A. H. (2016) Coinhibitory Pathways in the B7-CD28 Ligand-Receptor Family. *Immunity* **44**, 955-972
2. Baumeister, S. H., Freeman, G. J., Dranoff, G., and Sharpe, A. H. (2016) Coinhibitory Pathways in Immunotherapy for Cancer. *Annu Rev Immunol* **34**, 539-573
3. Iwai, Y., Ishida, M., Tanaka, Y., Okazaki, T., Honjo, T., and Minato, N. (2002) Involvement of PD-L1 on tumor cells in the escape from host immune system and tumor immunotherapy by PD-L1 blockade. *Proc Natl Acad Sci U S A* **99**, 12293-12297
4. Barber, D. L., Wherry, E. J., Masopust, D., Zhu, B., Allison, J. P., Sharpe, A. H., Freeman, G. J., and Ahmed, R. (2006) Restoring function in exhausted CD8 T cells during chronic viral infection. *Nature* **439**, 682-687
5. Day, C. L., Kaufmann, D. E., Kiepiela, P., Brown, J. A., Moodley, E. S., Reddy, S., et al.,. (2006) PD-1 expression on HIV-specific T cells is associated with T-cell exhaustion and disease progression. *Nature* **443**, 350-354
6. Freeman, G. J., Long, A. J., Iwai, Y., Bourque, K., Chernova, T., Nishimura, H. et al., (2000) Engagement of the PD-1 immunoinhibitory receptor by a novel B7 family member leads to negative regulation of lymphocyte activation. *J Exp Med* **192**, 1027-1034
7. Okazaki, T., Iwai, Y., and Honjo, T. (2002) New regulatory co-receptors: inducible co-stimulator and PD-1. *Curr Opin Immunol* **14**, 779-782
8. Latchman, Y., Wood, C. R., Chernova, T., Chaudhary, D., Borde, M., Chernova, I., et al., (2001) PD-L2 is a second ligand for PD-1 and inhibits T cell activation. *Nature immunology* **2**, 261-268
9. Topalian, S. L., Hodi, F. S., Brahmer, J. R., Gettinger, S. N., Smith, D. C., McDermott, D. F., et al., (2012) Safety, activity, and immune correlates of anti-PD-1 antibody in cancer. *The New England journal of medicine* **366**, 2443-2454
10. Wolchok, J. D., Kluger, H., Callahan, M. K., Postow, M. A., Rizvi, N. A., Lesokhin, A. etv al.. (2013) Nivolumab plus ipilimumab in advanced melanoma. *The New England journal of medicine* **369**, 122-133
11. Ahmadzadeh, M., Johnson, L. A., Heemskerk, B., Wunderlich, J. R., Dudley, M. E., White, D. E., and Rosenberg, S. A. (2009) Tumor antigen-specific CD8 T cells infiltrating the tumor express high levels of PD-1 and are functionally impaired. *Blood* **114**, 1537-1544

12. Ghebeh, H., Mohammed, S., Al-Omair, A., Qattan, A., Lehe, C., Al-Qudaihi, G., et al., (2006) The B7-H1 (PD-L1) T lymphocyte-inhibitory molecule is expressed in breast cancer patients with infiltrating ductal carcinoma: correlation with important high-risk prognostic factors. *Neoplasia* **8**, 190-198
13. Krueger, J., and Rudd, C. E. (2017) Two Strings in One Bow: PD-1 Negatively Regulates via Co-receptor CD28 on T Cells. *Immunity* **46**, 529-531
14. Kamphorst, A. O., Wieland, A., Nasti, T., Yang, S., Zhang, R., Barber, D. L., et al., (2017) Rescue of exhausted CD8 T cells by PD-1-targeted therapies is CD28-dependent. *Science* **355**, 1423-1427
15. Hui, E., Cheung, J., Zhu, J., Su, X., Taylor, M. J., Wallweber, H. A., et al., (2017) T cell costimulatory receptor CD28 is a primary target for PD-1-mediated inhibition. *Science* **355**, 1428-1433
16. Staron, M. M., Gray, S. M., Marshall, H. D., Parish, I. A., Chen, J. H., Perry, C. J., et al., (2014) The transcription factor FoxO1 sustains expression of the inhibitory receptor PD-1 and survival of antiviral CD8(+) T cells during chronic infection. *Immunity* **41**, 802-814
17. Oestreich, K. J., Yoon, H., Ahmed, R., and Boss, J. M. (2008) NFATc1 regulates PD-1 expression upon T cell activation. *Journal of immunology* **181**, 4832-4839
18. Mathieu, M., Cotta-Grand, N., Daudelin, J. F., Thebault, P., and Labrecque, N. (2013) Notch signaling regulates PD-1 expression during CD8(+) T-cell activation. *Immunology and cell biology* **91**, 82-88
19. Xiao, G., Deng, A., Liu, H., Ge, G., and Liu, X. (2012) Activator protein 1 suppresses antitumor T-cell function via the induction of programmed death 1. *Proceedings of the National Academy of Sciences of the United States of America* **109**, 15419-15424
20. Weiss, A., and Littman, D. R. (1994) Signal transduction by lymphocyte antigen receptors. *Cell* **76**, 263-274
21. Rudd, C. E. (1999) Adaptors and molecular scaffolds in immune cell signaling. *Cell* **96**, 5-8
22. Rudd, C. E., Trevillyan, J. M., Dasgupta, J. D., Wong, L. L., and Schlossman, S. F. (1988) The CD4 receptor is complexed in detergent lysates to a protein-tyrosine kinase (pp58) from human T lymphocytes. *Proc Natl Acad Sci U S A* **85**, 5190-5194
23. Barber, E. K., Dasgupta, J. D., Schlossman, S. F., Trevillyan, J. M., and Rudd, C. E. (1989) The CD4 and CD8 antigens are coupled to a protein-tyrosine kinase (p56lck) that phosphorylates the CD3 complex. *Proc Natl Acad Sci U S A* **86**, 3277-3281

24. Veillette, A., Bookman, M. A., Horak, E. M., Samelson, L. E., and Bolen, J. B. (1989) Signal transduction through the CD4 receptor involves the activation of the internal membrane tyrosine-protein kinase p56lck. *Nature* **338**, 257-259
25. Chan, A. C., Iwashima, M., Turck, C. W., and Weiss, A. (1992) ZAP-70: a 70 kd protein-tyrosine kinase that associates with the TCR zeta chain. *Cell* **71**, 649-662
26. Woodgett, J. R. (1990) Molecular cloning and expression of glycogen synthase kinase-3/factor A. *The EMBO journal* **9**, 2431-2438
27. Cohen, P., and Frame, S. (2001) The renaissance of GSK3. *Nat Rev Mol Cell Biol* **2**, 769-776
28. Beals, C. R., Sheridan, C. M., Turck, C. W., Gardner, P., and Crabtree, G. R. (1997) Nuclear export of NF-ATc enhanced by glycogen synthase kinase-3. *Science* **275**, 1930-1934
29. Neal, J. W., and Clipstone, N. A. (2001) Glycogen synthase kinase-3 inhibits the DNA binding activity of NFATc. *J Biol Chem*, 3666-3673
30. Ohteki, T., Parsons, M., Zakarian, A., Jones, R. G., Nguyen, L. T., Woodgett, J. R., and Ohashi, P. S. (2000) Negative regulation of T cell proliferation and interleukin 2 production by the serine threonine kinase GSK-3. *J Exp Med* **192**, 99-104
31. Wood, J. E., Schneider, H., and Rudd, C. E. (2006) TcR and TcR-CD28 engagement of protein kinase B (PKB/AKT) and glycogen synthase kinase-3 (GSK-3) operates independently of guanine nucleotide exchange factor VAV-1. *J Biol Chem* **281**, 32385-32394
32. Appleman, L. J., van Puijenbroek, A. A., Shu, K. M., Nadler, L. M., and Boussiotis, V. A. (2002) CD28 costimulation mediates down-regulation of p27kip1 and cell cycle progression by activation of the PI3K/PKB signaling pathway in primary human T cells. *J Immunol* **168**, 2729-2736
33. Jope, R. S., and Roh, M. S. (2006) Glycogen synthase kinase-3 (GSK3) in psychiatric diseases and therapeutic interventions. *Curr Drug Targets* **7**, 1421-1434
34. Mazanetz, M. P., and Fischer, P. M. (2007) Untangling tau hyperphosphorylation in drug design for neurodegenerative diseases. *Nat Rev Drug Discov* **6**, 464-479
35. Tolosa, E., Litvan, I., Hoglinger, G. U., Burn, D., Lees, A., Andres, M. V. et al., (2014) A phase 2 trial of the GSK-3 inhibitor tideglusib in progressive supranuclear palsy. *Mov Disord* **29**, 470-478
36. Taylor, A., Harker, J. A., Chanthong, K., Stevenson, P. G., Zuniga, E. I., and Rudd, C. E. (2016) Glycogen synthase kinase 3 inactivation drives T-bet-mediated

- downregulation of co-receptor PD-1 to enhance CD8(+) cytolytic T cell responses. *Immunity* **44**, 274-286
37. Boissonnas, A., Fetler, L., Zeelenberg, I. S., Hugues, S., and Amigorena, S. (2007) In vivo imaging of cytotoxic T cell infiltration and elimination of a solid tumor. *J Exp Med* **204**, 345-356
38. Lazarevic, V., and Glimcher, L. H. (2011) T-bet in disease. *Nat Immunol* **12**, 597-606
39. Grundy, M. A., Zhang, T., and Sentman, C. L. (2007) NK cells rapidly remove B16F10 tumor cells in a perforin and interferon-gamma independent manner in vivo. *Cancer Immunol Immunother* **56**, 1153-1161
40. McMillan, T. J., Rao, J., Everett, C. A., and Hart, I. R. (1987) Interferon-induced alterations in metastatic capacity, class-1 antigen expression and natural killer cell sensitivity of melanoma cells. *Int J Cancer* **40**, 659-663
41. Takeda, K., Nakayama, M., Sakaki, M., Hayakawa, Y., Imawari, M., Ogasawara, K. et al., (2011) IFN-gamma production by lung NK cells is critical for the natural resistance to pulmonary metastasis of B16 melanoma in mice. *J Leukoc Biol* **90**, 777-785
42. Parameswaran, R., Ramakrishnan, P., Moreton, S. A., Xia, Z., Hou, Y., Lee, D. A., et al., (2016) Repression of GSK3 restores NK cell cytotoxicity in AML patients. *Nat Commun* **7**, 11154
43. Gill, S., and June, C. H. (2015) Going viral: chimeric antigen receptor T-cell therapy for hematological malignancies. *Immunol Rev* **263**, 68-89
44. Zhu, Q., Yang, J., Han, S., Liu, J., Holzbeierlein, J., Thrasher, J. B., and Li, B. (2011) Suppression of glycogen synthase kinase 3 activity reduces tumor growth of prostate cancer in vivo. *Prostate* **71**, 835-845
45. Klein, P. S., and Melton, D. A. (1996) A molecular mechanism for the effect of lithium on development. *Proc Natl Acad Sci U S A* **93**, 8455-8459
46. Piazza, F., Manni, S., Tubi, L. Q., Montini, B., Pavan, L., Colpo, A., et al., (2010) Glycogen Synthase Kinase-3 regulates multiple myeloma cell growth and bortezomib-induced cell death. *BMC Cancer* **10**, 526
47. Dickey, A., Schleicher, S., Leahy, K., Hu, R., Hallahan, D., and Thotala, D. K. (2011) GSK-3beta inhibition promotes cell death, apoptosis, and in vivo tumor growth delay in neuroblastoma Neuro-2A cell line. *J Neurooncol* **104**, 145-153
48. Beurel, E., Blivet-Van Eggelpoel, M. J., Kornprobst, M., Moritz, S., Delelo, R., Paye, F., et al., (2009) Glycogen synthase kinase-3 inhibitors augment TRAIL-induced apoptotic death in human hepatoma cells. *Biochem Pharmacol* **77**, 54-65

49. Finke, J. H., Zea, A. H., Stanley, J., Longo, D. L., Mizoguchi, H., Tubbs, R. R. et al., (1993) Loss of T-cell receptor zeta chain and p56lck in T-cells infiltrating human renal cell carcinoma. *Cancer Res* **53**, 5613-5616
50. Rayman, P., Uzzo, R. G., Kolenko, V., Bloom, T., Cathcart, M. K., Molto, L. et al., (2000) Tumor-induced dysfunction in interleukin-2 production and interleukin-2 receptor signaling: a mechanism of immune escape. *Cancer J Sci Am* **6 Suppl 1**, S81-87

## Figures

### Figure 1. GSK-3 inhibition, anti-PD-1 and combination reduce pulmonary metastasis of B16

**melanoma to the same extent.** (A) Schematic representation of treatment regime (left upper panel). Histogram showing the number of lung spots per animal with or without the described treatment (right panel), photograph below shows 1 example of each group (n=6 mice per condition). (B) Flow cytometric profiles of PD-1 expression for T cells isolated from spleen, draining lymph nodes and tumor infiltrating lymph nodes (TILs) (data representative of 6 samples). (C) Quantitative real-time PCR of PD-1 and T-bet transcription of splenic T cells. (D) % of CD8<sup>+</sup> cells expressing granzyme B of tumor infiltrating cells as determined by flow cytometry (n=6)\*\*, P < 0.001. (E) Dose response of SB415286 on B16 melanoma. C57/bl6 mice were injected intravenously with luciferase tagged B16 melanoma cells and treated with doses of SB41586 as indicated. Luminescent images show B16 metastasis at day 14 and flow cytometric profiles to the right of each image show the level of PD1 expression on different cell subsets, taken from the spleen at day 14 (n=3).

### Figure 2. Pulmonary metastasis of B16 melanoma is reduced to the same extent in *GSK-3 $\alpha/\beta$*

*-/-* and *Pdcd*<sup>-/-</sup> mice. (A) CD8<sup>+</sup> T-cells from *GSK-3 $\alpha/\beta$* <sup>-/-</sup> mice show a decrease in PD-1 expression relative to CD8<sup>+</sup> T-cells from wild-type control mice (left) CD8<sup>+</sup> T-cells (Right) CD4<sup>+</sup> T-cells. (B) *GSK-3 $\alpha/\beta$* <sup>-/-</sup> enhanced clearance of lung melanoma. Upper inset: expanded abscissa range showing a lack of an effect of anti-PD-1 on numbers of nodules in *GSK-3 $\alpha/\beta$* <sup>-/-</sup> mice (n=5 mice per condition). \*, P < 0.05; \*\*, P < 0.001; ns, no significant difference relative to controls. (C) *Pdcd*<sup>-/-</sup> mice show enhanced clearance of lung B16 melanoma. Upper right inset: expanded abscissa range showing a lack of an effect of GSK-3 inhibitors SB415286 and AZ1080 on numbers of B16 nodules in *Pdcd*<sup>-/-</sup> mice. (n=5 mice per condition). Panel shows a representative experiment. \*, P < 0.05; \*\*, P < 0.001; ns, no significant difference relative to controls. (D) Inhibition of GSK-3 does not affect pulmonary metastasis of B16 melanoma in *Rag2*<sup>-/-</sup> mice. Left panel: photo of lungs harvested from

Rag2<sup>-/-</sup> mice 14 days after injection of B16 cells in the presence or absence of the injection of 6 doses of 200 $\mu$ g SB415286. Right panel: histogram shows number of spots from mice in left panel (n=3).

**Figure 3. GSK-3 inhibition and anti-PD-1 enhance clearance of established B16 tumors**

(A) Schematic representation of treatment regime (upper left panel). Histogram showing the number of lung spots per animal with or without the described treatment (right panel), Photograph below shows 1 example of each group. (n=6 mice per condition). (B) Quantitative real-time PCR of PD-1 and T-bet transcription of splenic T cells from animals used in (A) (n=5). \*, P < 0.05; \*\*, P < 0.001; ns, no significant difference relative to controls. (C) Flow cytometric profiles of PD-1 expression on T cells isolated from spleen and TILs (data representative of 5 samples). (D) % of CD8<sup>+</sup> cells expressing granzyme B of tumor infiltrating cells as determined by flow cytometry (n=5)

**Figure 4. GSK-3 inhibition and anti-PD-1 inhibit growth of solid B16 tumors.** (A) Schematic representation of treatment regime (upper panel); tumor growth curves (lower panels). Number in lower right corner represents how many mice (out of 3) from each treated condition were tumor free at the end of the study. (B) Survival curves of mice with and without treatment as shown (n=6; number of mice: 24). Panel shows a representative experiment. (C) Quantitative real-time PCR of splenic T-cells. (D) Flow cytometric profiles for T-cells isolated from draining lymph nodes and TILs (data representative of 5 samples). (E) Quantitative real-time PCR of tumor infiltrating lymphocytes. (F) % of CD8<sup>+</sup> cells expressing CD107a/granzyme B (GZMB) of tumor infiltrating cells as determined by flow cytometry. \*\*P < 0.001; ns, no significant difference relative to controls.

**Figure 5. GSK-3 inhibition and anti-PD-1/PL1 attenuate growth to a similar extent of solid EL4-OVA tumors.** (A) GSK-3 inhibition enhances clearance of solid EL4-OVA tumors. (Top panel) Schematic representation of treatment regime for EL4 solid tumor model with different

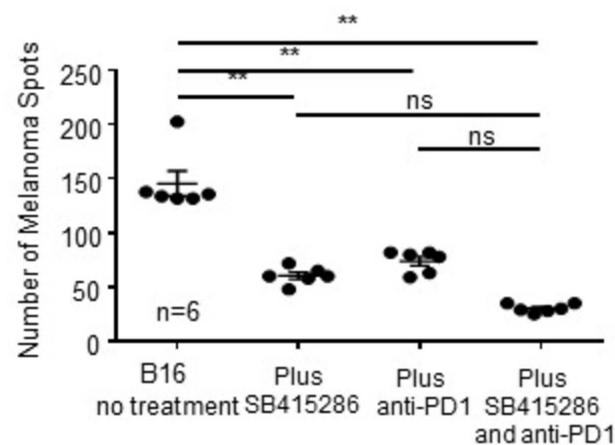
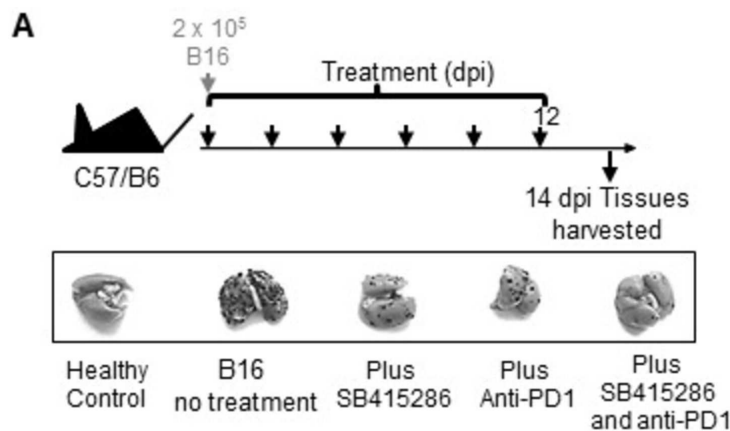
concentrations of OVA peptide. Non-OVA pulsed EL4 cells were injected into the left flank and EL4-OVA cells into the right flank. (Middle panel) Photograph showing tumor growth after 10 days of OVA-pulsed EL4 tumor cells in OT-1 Tg mice with or without SB415286 injection (upper panel). (Lower panel) Tumor growth curves (n=6 mice per condition). Panel shows a representative experiment. (B) Real time PCR of splenic T-cells confirmed SB415286 inhibition of PD-1 and Tbet transcription. Flow cytometric profile of anti-PD-1 staining of spleen T-cells. (C) SB415286 and anti-PD-1 alone and in combination attenuate B16 cell growth (upper panels). Lower panel: SB415286 and anti-PD-1 alone and in combination increased mouse survival to the same degree. 2ug OVA peptide (lower left panel); 5ug OVA peptide (lower middle panel); 10ug/ml (lower right panel). Number in lower right corner represents how many mice (out of 6) were tumor free at the end of the study. (D) SB415286, anti-PD-1 and anti-PD L-1 (PD-1 ligand) show a similar effect on the inhibition of EL4 tumor growth (upper panels). Left panel: effects in the presence of 5ug OVA peptide; Right panel: effects in the presence of 10ug OVA peptide. Number in lower right corner represents how many mice (out of 3) from each treated condition were tumor free at the end of the study. Lower panel: Quantitative real-time PCR of PD-1 and T-bet transcription.

**Figure 6. GSK-3 inhibition and combined anti-PD-1 therapy slows solid EL4 tumor growth.**

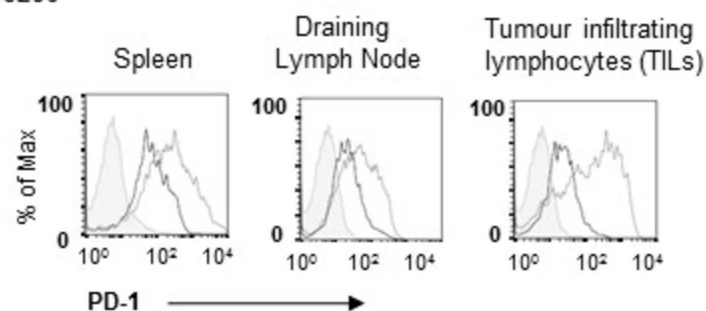
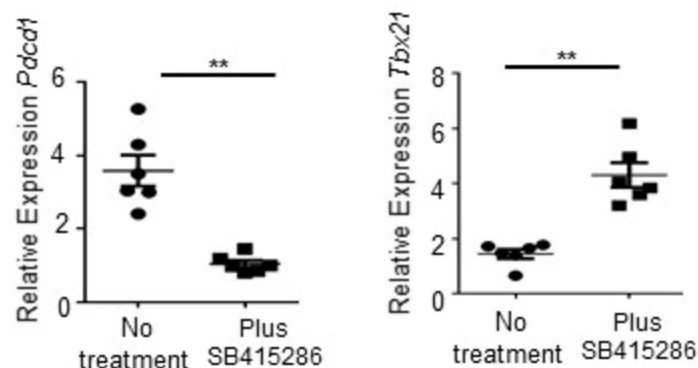
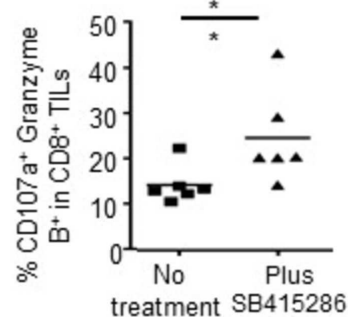
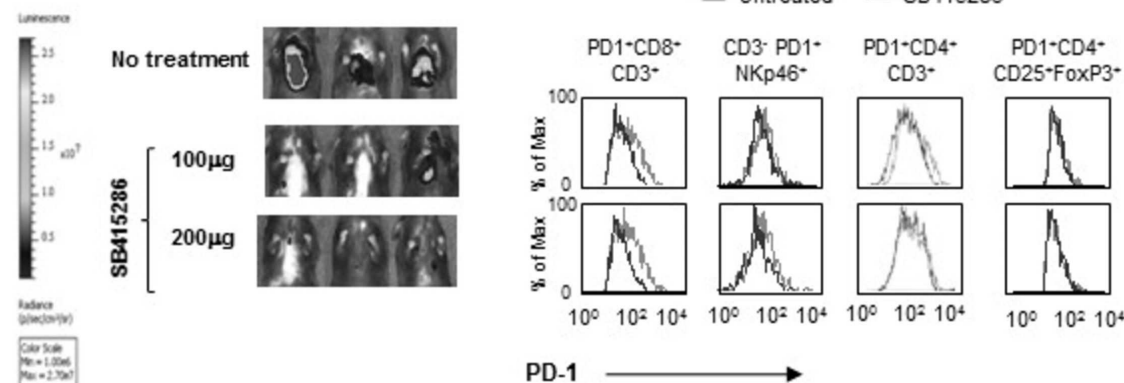
(A) Schematic representation of treatment regime for EL4 solid tumor model without OVA-presentation (upper panel). Tumor growth curves (lower panels) (n=6 mice per condition). Number in lower right corner represents how many mice (out of 6) were tumor free at the end of the study. (B) Survival curves. (C) Flow cytometric profiles of PD-1 expression, data representative of 5 samples. (D) Quantitative real-time PCR of PD-1 and T-bet transcription (n=5).

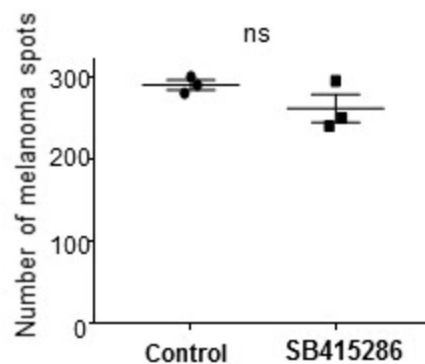
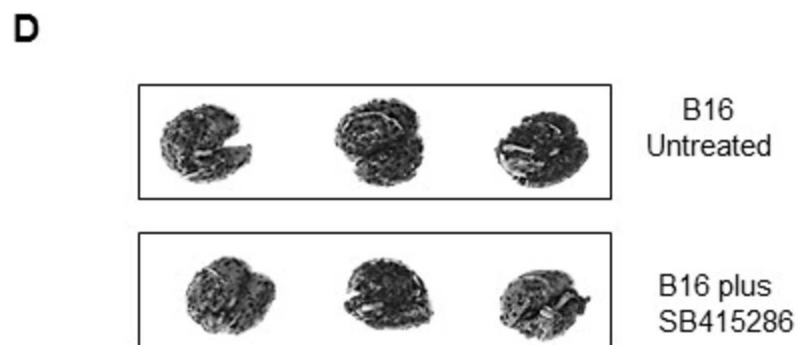
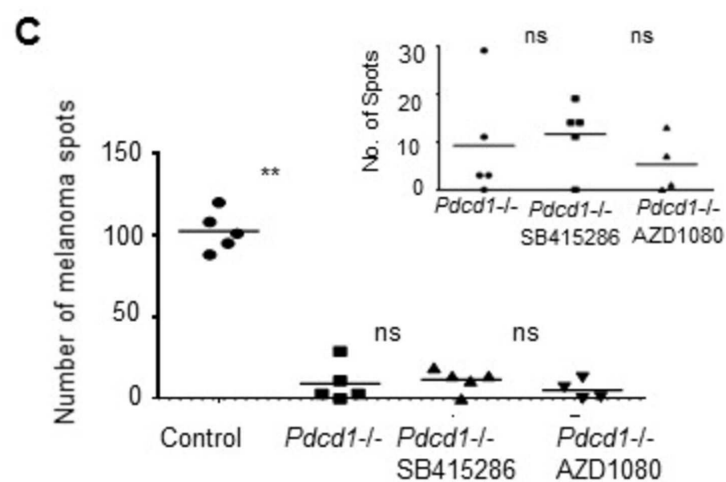
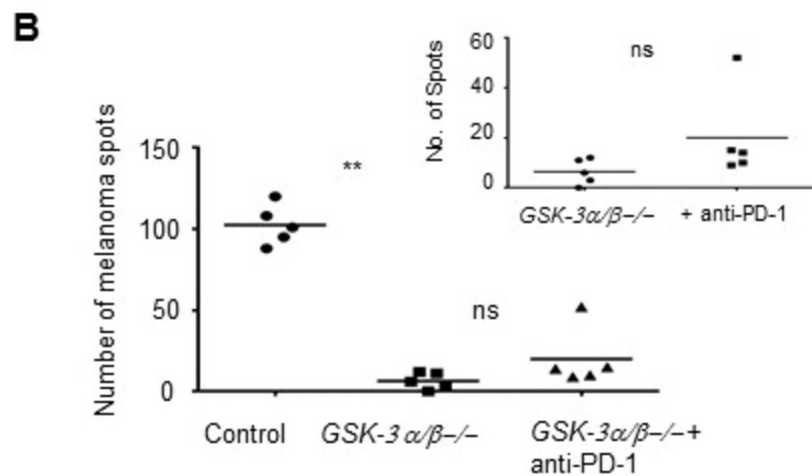
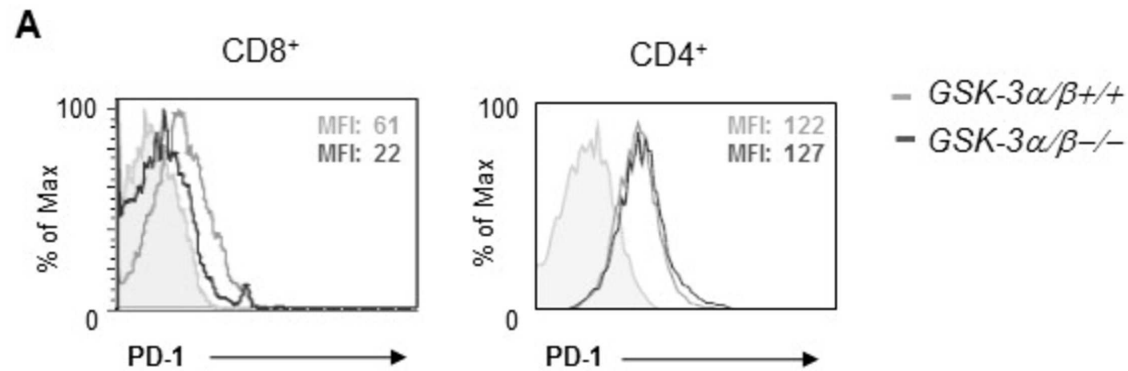
**Figure 7. Ex vivo pre-treatment of T-cells with SB415286, anti-PD-1 or combination followed by adoptive therapy delayed the onset EL4-OVA tumor growth.** (A) Regime of adoptive therapy

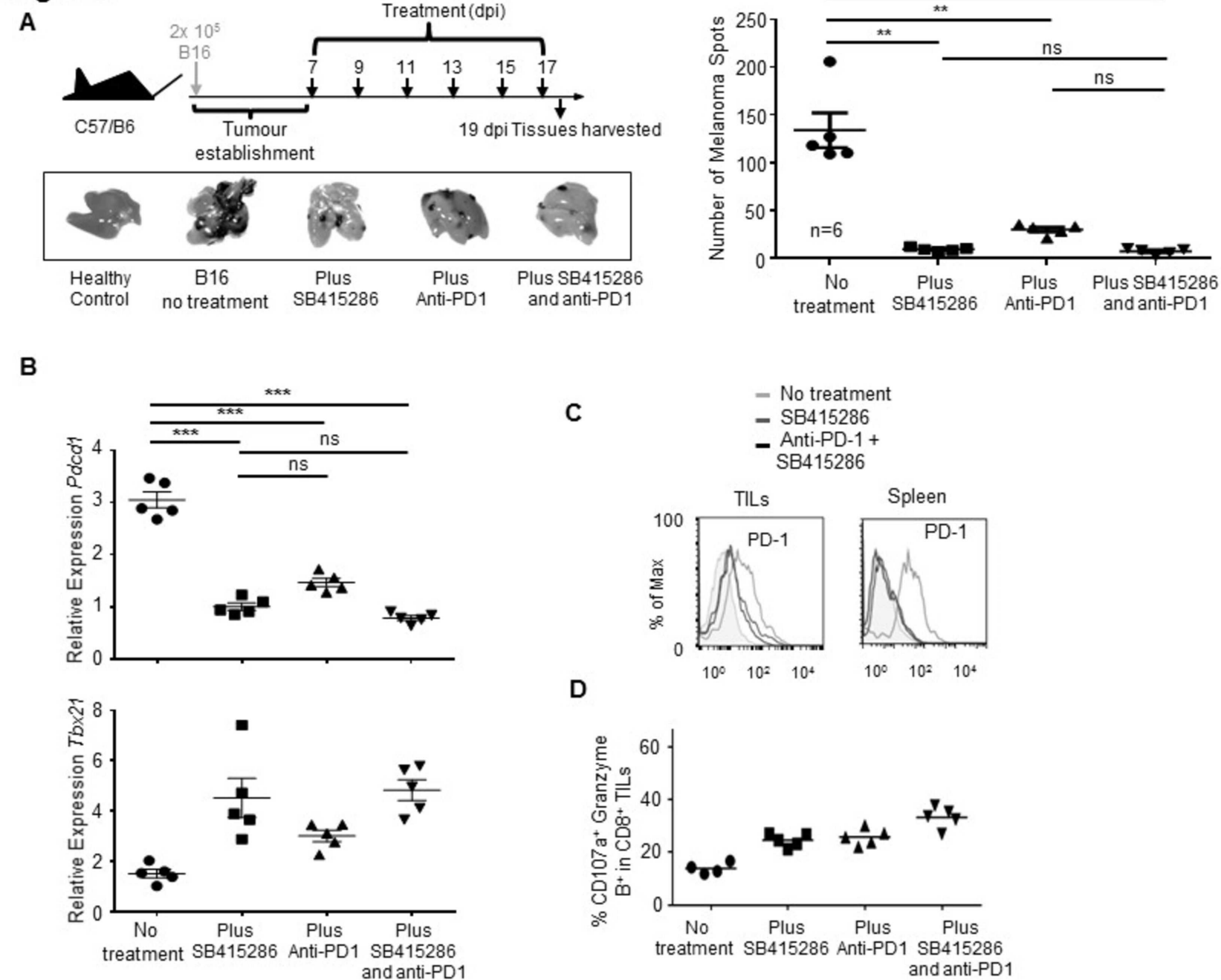
(upper panel). Tumor growth curves (n=3; number of mice: >20) (lower panels). Panel shows a representative experiment. Number in lower right corner represents how many mice (out of 3) from each treated condition were tumor free at the end of the study. (B) Real time PCR of splenic T-cells prior to adoptive transfer confirmed SB415286 inhibition of PD-1 and Tbet transcription (upper panels). (C) Flow cytometric profiles of anti-PD-1 staining of spleen T-cells treated with different concentrations of OVA peptide prior to adoptive transfer.

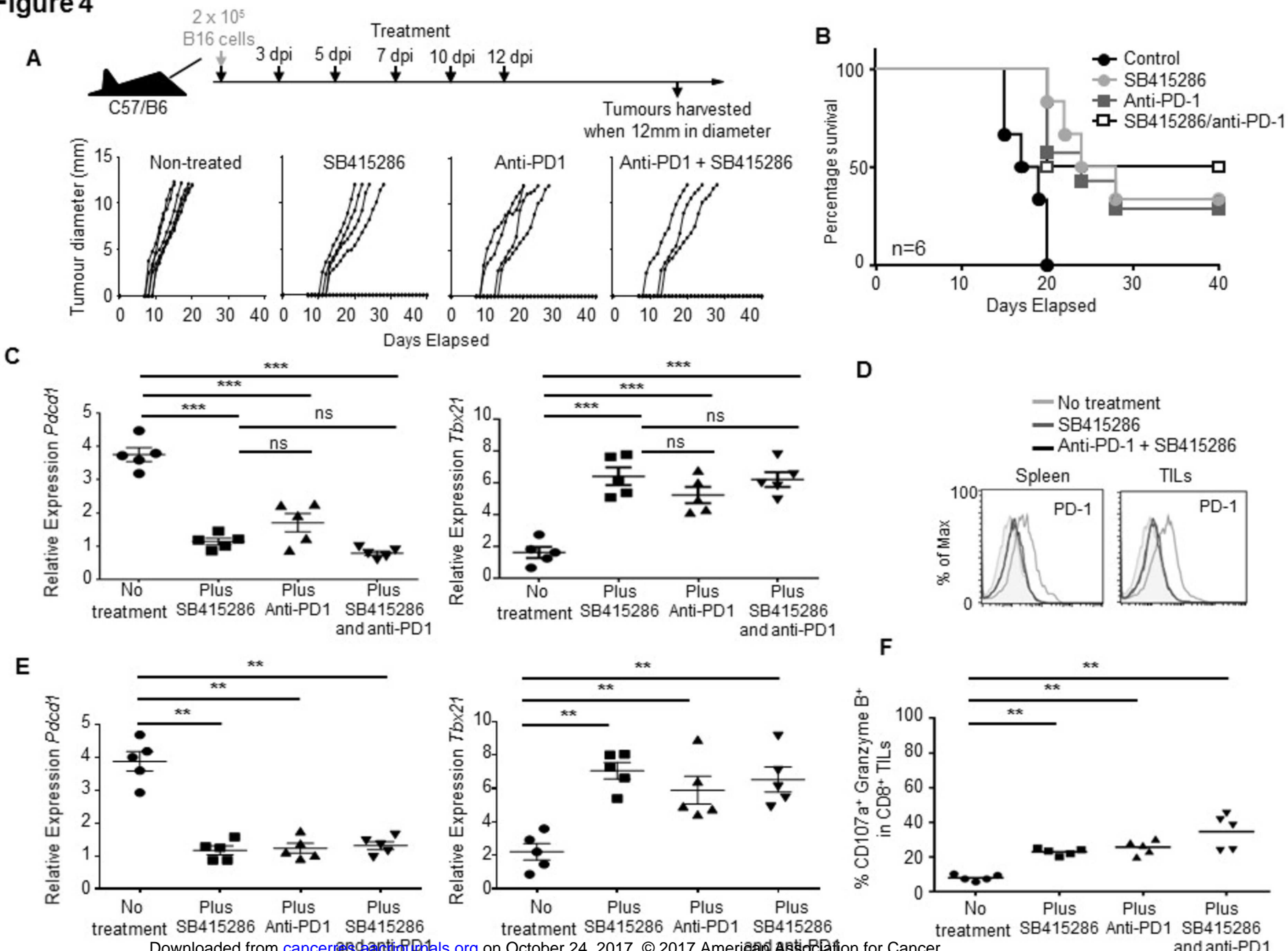
**Figure 1****B**

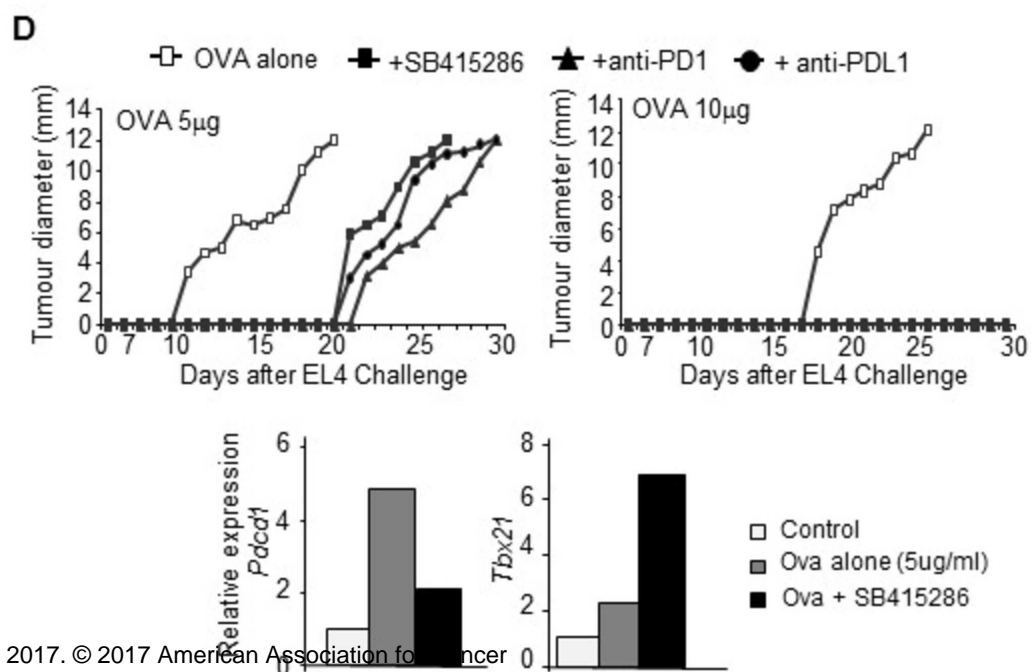
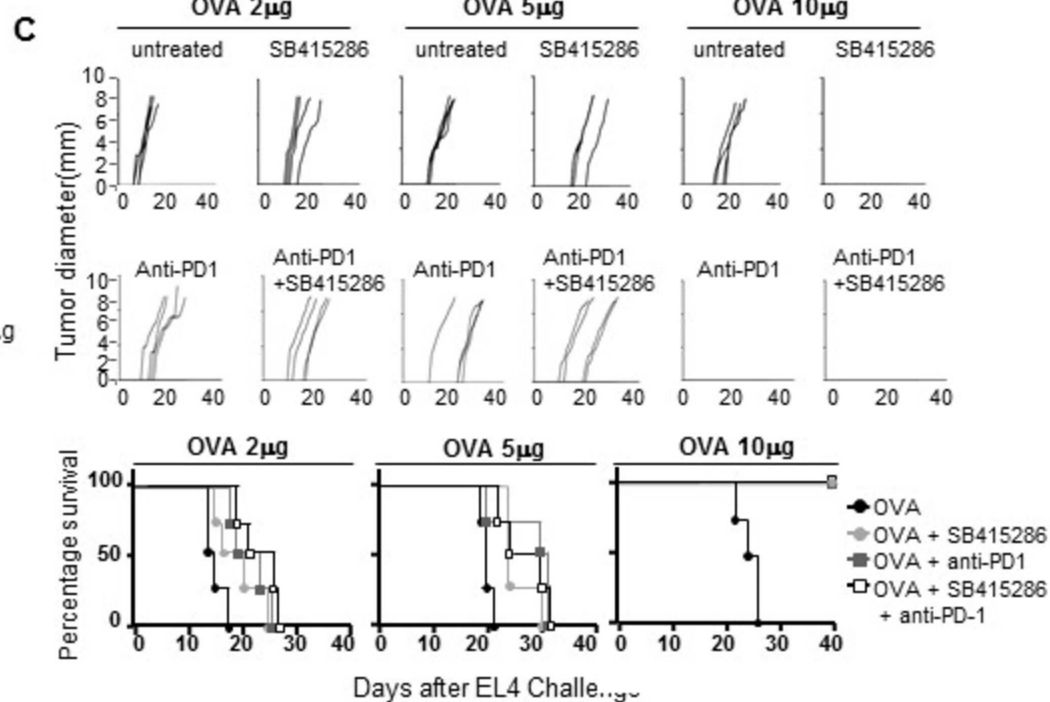
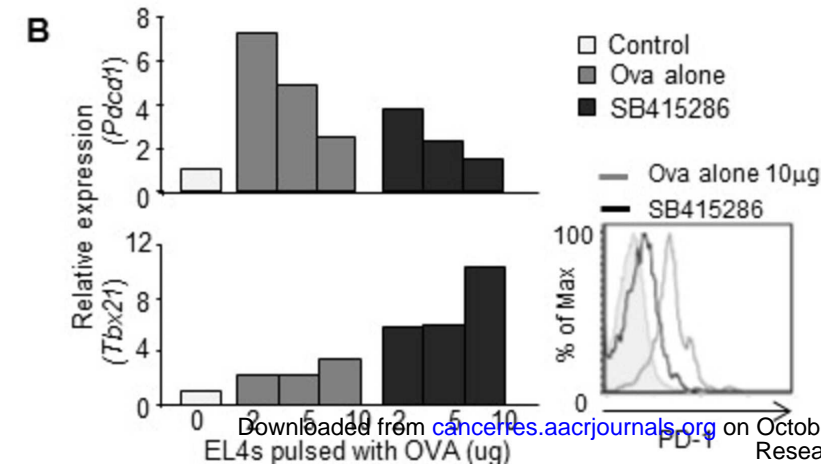
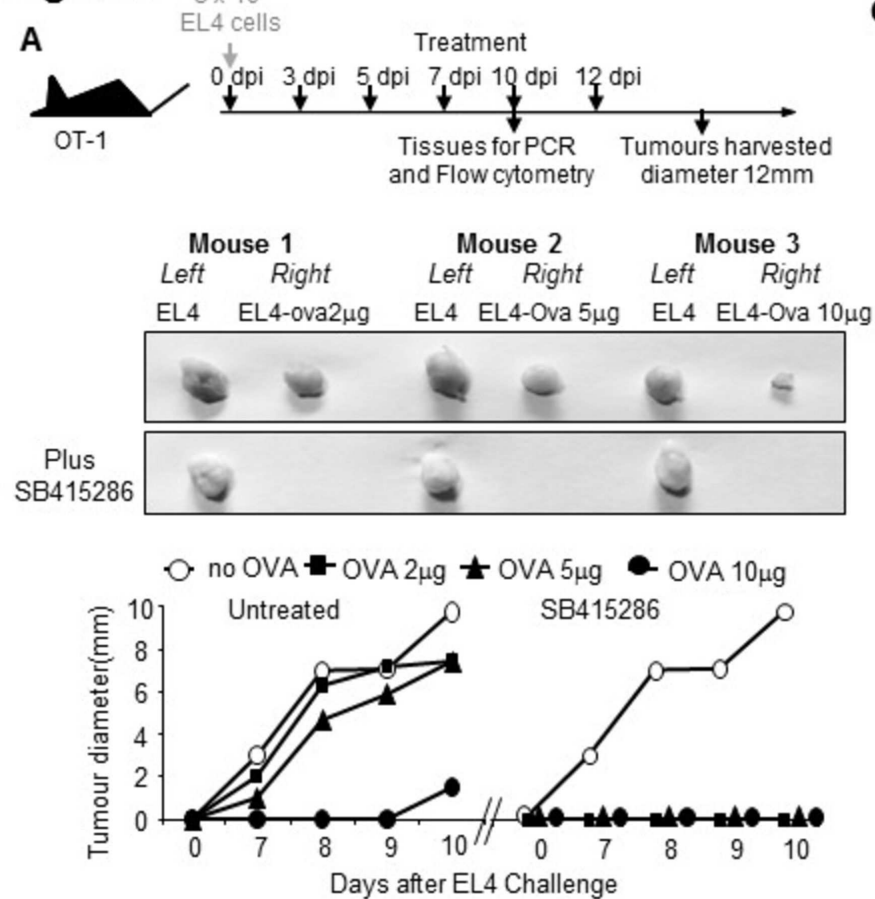
- No treatment
- SB415286

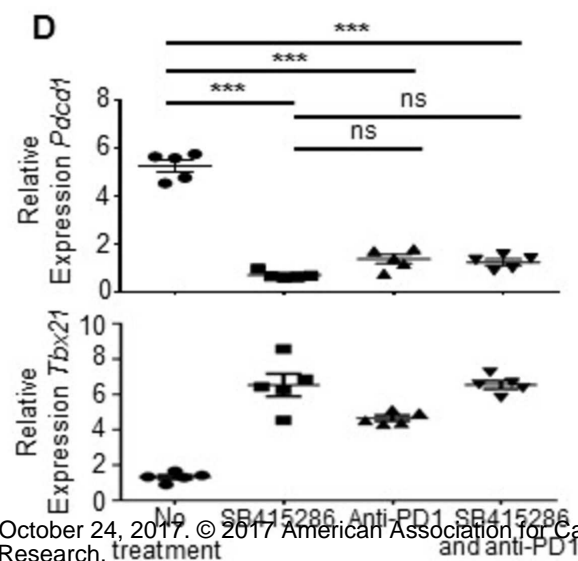
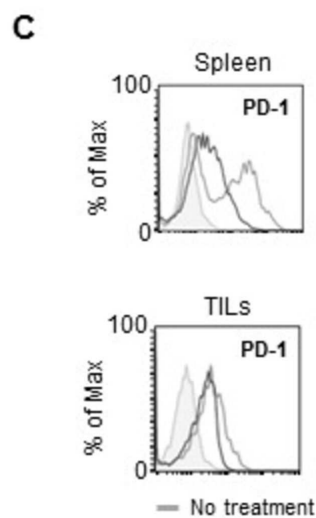
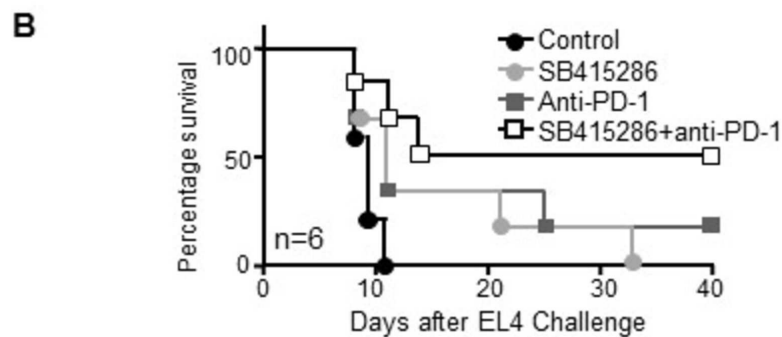
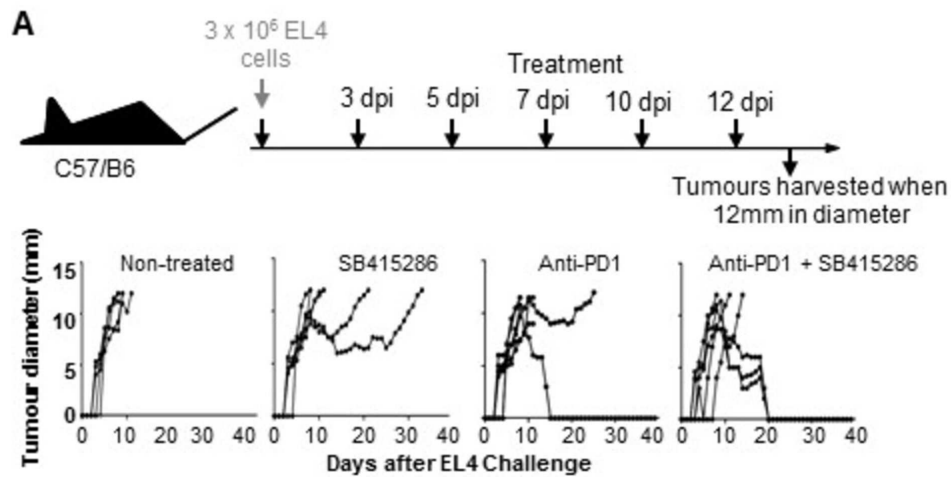
**C****D****E**

**Figure 2**

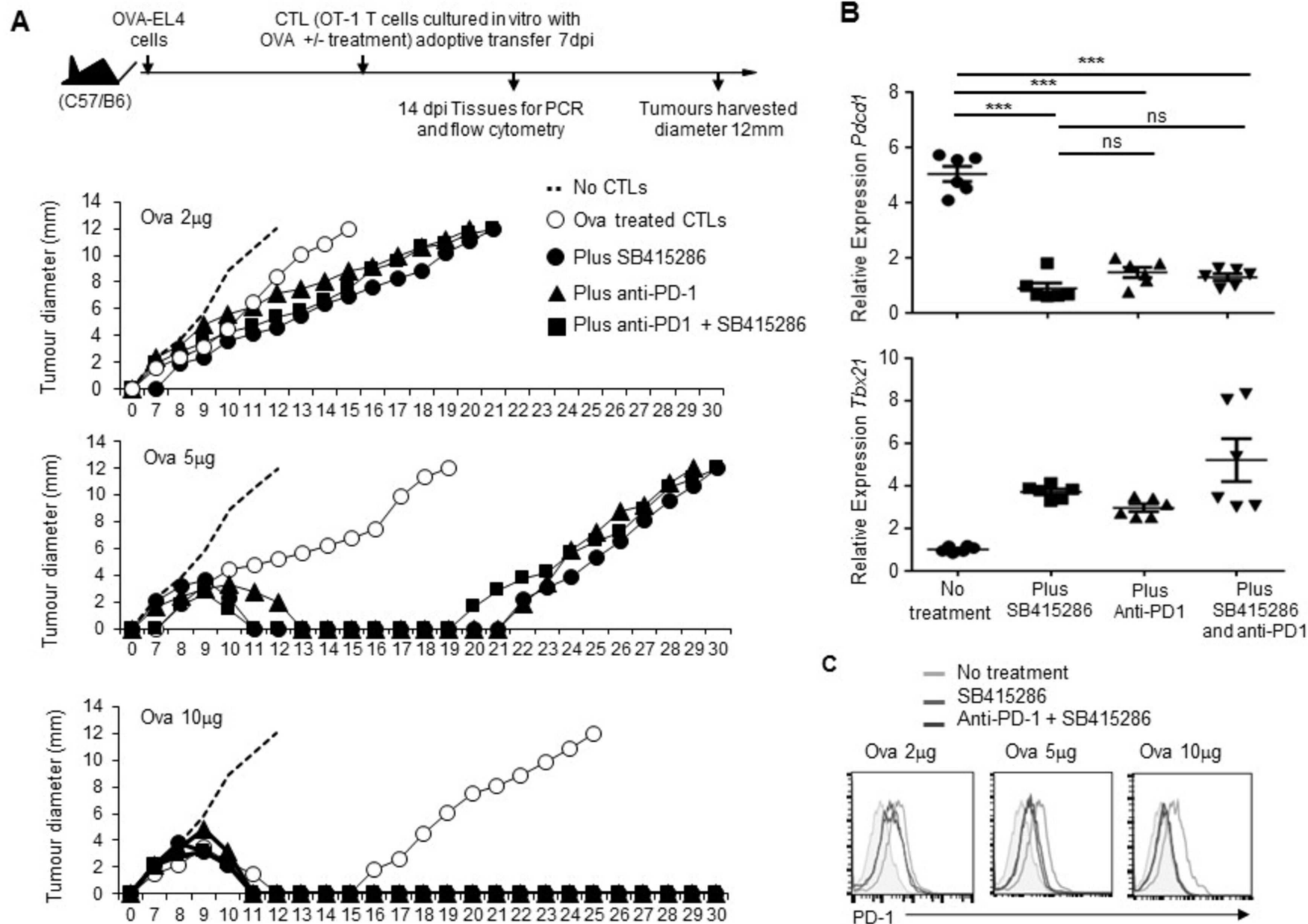
**Figure 3**

**Figure 4**

**Figure 5**

**Figure 6**

**Figure 7**



# Cancer Research

The Journal of Cancer Research (1916–1930) | The American Journal of Cancer (1931–1940)

## Small molecule inhibition of PD-1 transcription is an effective alternative to antibody blockade in cancer therapy

Alison Taylor, David Rothstein and Christopher Rudd

*Cancer Res* Published OnlineFirst October 20, 2017.

<b>Updated version</b>	Access the most recent version of this article at: doi: <a href="https://doi.org/10.1158/0008-5472.CAN-17-0491">10.1158/0008-5472.CAN-17-0491</a>
<b>Supplementary Material</b>	Access the most recent supplemental material at: <a href="http://cancerres.aacrjournals.org/content/suppl/2017/10/20/0008-5472.CAN-17-0491.DC1">http://cancerres.aacrjournals.org/content/suppl/2017/10/20/0008-5472.CAN-17-0491.DC1</a>
<b>Author Manuscript</b>	Author manuscripts have been peer reviewed and accepted for publication but have not yet been edited.

**E-mail alerts** [Sign up to receive free email-alerts](#) related to this article or journal.

**Reprints and Subscriptions** To order reprints of this article or to subscribe to the journal, contact the AACR Publications Department at [pubs@aacr.org](mailto:pubs@aacr.org).

**Permissions** To request permission to re-use all or part of this article, contact the AACR Publications Department at [permissions@aacr.org](mailto:permissions@aacr.org).